



Compatibilising action of multiwalled carbon nanotubes in polycarbonate/polypropylene (PC/PP) blends: phase morphology, viscoelastic phase separation, rheology and percolation

Mohammed Arif Poothanari¹ · Priti Xavier² · Suryasarathi Bose² · Nandakumar Kalarikkal^{1,3} · Cibi Komalan⁴ · Sabu Thomas^{1,5}

Received: 15 October 2018 / Accepted: 11 June 2019 / Published online: 2 July 2019

© The Polymer Society, Taipei 2019

Abstract

Multiwalled carbon nanotubes were introduced into both dispersed and co-continuous polycarbonate/polypropylene blends through melt compounding in an internal mixer. Both the neat blends and blend nanocomposites showed viscoelastic phase separation process where phase in phase morphologies could be observed due to viscosity disparity and T_g differences between the component polymers. A strong compatibilising action was noticed up on the addition of a small quantity of MWCNT into both dispersed and co-continuous morphologies. Theoretical predictions based on thermodynamic considerations clearly indicated the preferential localisation of MWCNTs in the PC phase. However, because of the viscosity differences between the two polymers, we also found that some of the MWCNTs being localised at the blend interphase and in PP phase. From linear viscoelastic studies rheological percolation was observed at high concentration of the MWCNTs where carbon nanotubes formed a network-like structure leading to solid state behaviour at low frequencies.

Keywords Polycarbonate/polypropylene blends · Co-continuous morphology · Selective localization of MWCNTs

Introduction

Melt blending of polymers is an immensely attractive and inexpensive method of getting novel and different structural materials [1]. We can attain a good cost/performance ratio by the judicious mixing of low-cost polymers with expensive polymers. They can be

miscible or immiscible. The miscibility of polymer blend depends on the thermodynamics of mixing. Most of the blend systems are immiscible due to unfavorable interactions and very low contribution of entropy [2–4]. A wide range of morphologies (dispersed to co-continuous structures) could be obtained by carefully controlling the composition and viscosity ratio of immiscible polymer blends. In recent years, nanoparticles have attracted a lot of interest due to their important role in immiscible and incompatible polymer blends. The nanoparticles are able to change the interaction coefficient between two polymers and thus improve the compatibility between the polymer pairs [5]. The dispersed phase morphology (particle size less than 1 μm) improves the impact resistance of polymer systems and the co-continuous polymer blends are suitable for conductive and mechanical applications. In recent years, several researchers reported interesting studies on co-continuous polymer blend systems. Some of the papers describe the viscoelastic properties of co-continuous blends. Galloway et al. studied the co-

✉ Sabu Thomas
sabuthomas@mgu.ac.in; sabupolymer@yahoo.com

¹ International and Inter University Centre for Nanoscience and Nanotechnology, Mahatma Gandhi University, Kottayam, Kerala, India

² Materials Engineering Department, Indian Institute of Science, Bangalore, India

³ School of Pure and Applied Physics, Mahatma Gandhi University, Kottayam, Kerala, India

⁴ S.N.M. College, Maliankara, Kerala 683516, India

⁵ School of Chemical Sciences, Mahatma Gandhi University, Kottayam, Kerala, India

continuous morphology of PEO/PS blend system using the solvent extraction method [6]. Castro et al. reported on the rheological properties of co-continuous PEO/PVDF-HFP blend system [7]. The stabilisation of a co-continuous microstructure is very important in the application point of view. Many researchers have used the nanofillers to stabilise the co-continuous morphology of polymer/polymer blends [8–10]. They have used carbon black, carbon nanotubes, graphene, silica nanoparticles and nanoclay to stabilize the co-continuous blends.

The carbon nanotubes (CNTs) exhibit unique combination properties including good internal structure, high strength, stiffness and thermal and electrical conductivity [11]. They have recently received tremendous attention from scientific and industrial communities [12, 13]. The polymeric materials in general show advantages such as light weight, high strength, anti-rust, and ease of processability. CNT-based polymer nanocomposites exhibit good mechanical properties, morphology control and excellent conductivity characteristics [14]. Polymer nanocomposites containing CNTs are promising materials for high-performance application such as sensors [15], aerospace parts [16], electromagnetic shielding components [17, 18]. The reinforcing effect can be quantified through the percolation threshold. At the percolation threshold, the CNT-CNT network structure is achieved. At this concentration of CNTs, the rheological properties of the nanocomposites change from viscous fluid to solid like behaviour [19, 20]. When the concentration of conductive fillers reaches percolation threshold, the conductivity of the nanocomposites tremendously increases due to the formation of the conductive percolating network. The characteristics properties of CNT-based blend nanocomposites depends on the localisation of CNTs in the polymer phase. Potschke et al. reported that CNTs were selectively localised at the PC phase of polycarbonate/polyethylene (PC/PE) blend composite [21]. Ozcan et al. reported that CNT dispersed at PET component of PP/PET/CNT blend system [22]. Many researchers reported studies on the rheological properties of polymer blend with MWCNT [23–25]. Aref et al. analysed the effect of distribution and localisation of CNTs on the rheological and electrical properties of PA6/PP nanocomposites. They have reported that CNTs were dispersed in PA6 phase [26].

The rheological properties of these nanocomposites are very important as they affect the processing conditions. The rheological properties depend on the morphology of the materials, filler dispersion, the aspect ratio of nanotubes, and the interactions between filler and polymer matrix [27]. Polypropylene (PP)

and polycarbonate (PC) are thermoplastics having good mechanical properties and processability. PP is a semi-crystalline low-cost thermoplastic being used for a large number of applications in packaging, automotive, containers, etc. PC is an engineering thermoplastic being used in various fields like electronics, medical, optical media, etc. But the low heat resistance and poor low-temperature impact performance of PP restricts its application to a limited range of temperature. In order to overcome these drawbacks, blending of PP with a polymer having higher heat resistance and better impact is being practiced. Interestingly, polycarbonate (PC) is an expensive engineering thermoplastic having high heat and impact resistance and so the blending of PP with PC can provide a new blend system which could be used for many applications in an economical way [28]. However, the PC/PP blends are immiscible due to the viscosity mismatch (PP: low viscosity vs. PC: high viscosity) and polarity differences (PP: nonpolar vs. PC: polar). Although many studies have been reported on PC/PP blends [29, 30]. However, there is no systematic studies on the action of CNTs on the phase morphology and rheological behaviour of PC/PP blends. The influence of CNT and its concentration on the compatibilising action, phase co-continuity, refinement of the phase morphology and rheology have not been well understood.

In this work, we have carefully studied the morphological and rheological properties of PC/PP blend system in the presence and absence of MWCNT. The SEM, TEM and solvent extraction studies were used to analyse the microstructure of PC/PP blend systems. The effect of MWCNT loading on viscoelastic phase separation process was carefully investigated. Morphology-property correlation has been established.

Experimental

Materials

Polycarbonate (PC) (Makrolon® 6557- melt flow index = 1.2 g/10 min, Glass transition temperature (T_g) ~145 °C) was purchased from Bayer Material Science, Germany. The isotactic Polypropylene (iPP) (H350 FG- melt flow index = 38 g/10 min, Melting point (T_m) ~ 165 °C, Glass transition temperature (T_g) ~0–2 °C, crystallization temperature (T_c) ~110) was collected from Reliance, India Ltd., India. The multiwall carbon nanotube (MWCNT) (NC7000) was provided by Nanocyl, Belgium. The diameter of MWCNTs varies from 10 to 20 nm and the length ~ 1.5 μ m and 90% purity. Dichloromethane used in this study were of AR grade obtained from Merck Chemicals, India.

Sample preparation

All the blend composites were prepared by Brabender 33-internal melt mixer with a cavity size of 55 cm³ and chamber temperature of 230 °C. Melt blending was done at 60 rpm for 10 min. Prior to mixing, PC was dried at 120 °C in oven for 12 h to eliminate all moisture. The mixed sample is compression moulded at a temperature of 230 °C for 2 min and is cooled to room temperature at the same pressure (100 kg/cm²).

Solvent extraction

Circular sample disks of each blend were dipped in 200 ml of dichloromethane for 24 h for the dissolution of the PC phase. It was then kept in an oven at 80 °C and the weight of the disks after extraction was noted. The degree of continuity PC phase was evaluated based on its original weight and the change in weight during etching, by the eq. (1) [6]:

$$\Phi_i = \frac{m_{i0} - m_{if}}{m_{i0}} \quad (1)$$

where Φ_i is the degree of continuity of phase i , m_{i0} is the initial mass of phase i , and m_{if} is the mass of phase i after extraction. If the degree of continuity of each phase is 1.0, the system will be completely co-continuous.

Characterisations

The structural and rheological properties of the prepared sample have been carried out using different techniques.

Morphological studies

The morphologies of PC/PP blend were studied using Scanning Electron Microscopy (SEM) (JEOL- ESEM). The cryogenically fractured surface of the blend samples were analysed. The filler dispersion and morphological details of blend and nanocomposites were investigated by TEM (JEOL-2100 HRTEM). The samples for TEM analysis prepared using an ultra-microtome (Leica, Ultracut UCT).

Rheological measurements

Rheological properties were studied using Discovery Hybrid Rheometer 3 (TA instruments, USA) in stress controlled condition. The measurements were performed at 230 °C using 25 mm parallel plates geometry at a frequency range 0.1 to 100 rad/s.

Results and discussion

Morphology in the absence of multiwalled carbon nanotubes

SEM analysis was employed to study the morphology of PC/PP blends with and without the addition of MWCNT. The cryogenically fractured surface of the blend samples were used to SEM analysis. Figure 1 shows the SEM micrographs of blend systems. Phase separation between PC and PP has been observed, due to the immiscibility of PC/PP blends as reported earlier [31]. The glass transition temperatures of iPP and PC, crystallization of temperatures iPP may also affect the microstructure formation in the neat blend of PC/PP and nanotube/polymer blend composite. The morphology of blends was found to vary from dispersed to co-continuous followed by the phase inversion with the varying composition of the blend system. For the PC/PP (10/90) and PC/PP (30/70) blends, PC is the minor phase which is distributed as droplets in the PP matrix as shown Fig. 1.a and b. The PC/PP (60/40) blends formed co-continuous phase morphology, as shown in Fig. 1c. For PC/PP (70/30) blend, PP became the dispersed phase with different droplet shapes (Fig. 1.d). The Fig. 1.e shows SEM image of PC/PP (60/40) blend after the preferential etching of PC phase. The remaining PP phase forms continuous structure and from this, the co-continuous morphology is confirmed. The complete phase diagram is plotted in Fig. 2, where dispersed and co-continuous regions have been marked. It is very interesting to note that phase in phase morphology could be seen when the PC content is more than 30%. The careful examination of the fracture surface indicates droplets of PP in the continuous PC phase. It shows that PP particles are dispersed in the continuous PC phase and PC particles are dispersed in the continuous PP phase. Such a complex phase structure is associated with the viscoelastic phase separation process which is associated with the dynamic asymmetry arising from the differences in T_g and viscosity disparity between PP and PC phases [32]. The T_g of the PP phase is around 0 °C and that of PC phase is 145 °C. Additionally, the viscosity of PC phase is much higher than the PP phase as can be seen from the rheological data given in the later part of the paper. At mixing temperature, PP-rich phase shows more liquid-like behaviour and on the other hand, the PC-rich phase is under viscoelastic effect due to higher viscosity. In other words, the mobility disparity of the component polymers causes the viscoelastic phase separation process. Shi et al. reported similar phase separation process for PP/PMMA blends [33]. It is very important to add that we were the first group to report on the viscoelastic phase separation in PC/PP blends although this system was analysed by many research groups previously [29, 31, 34].

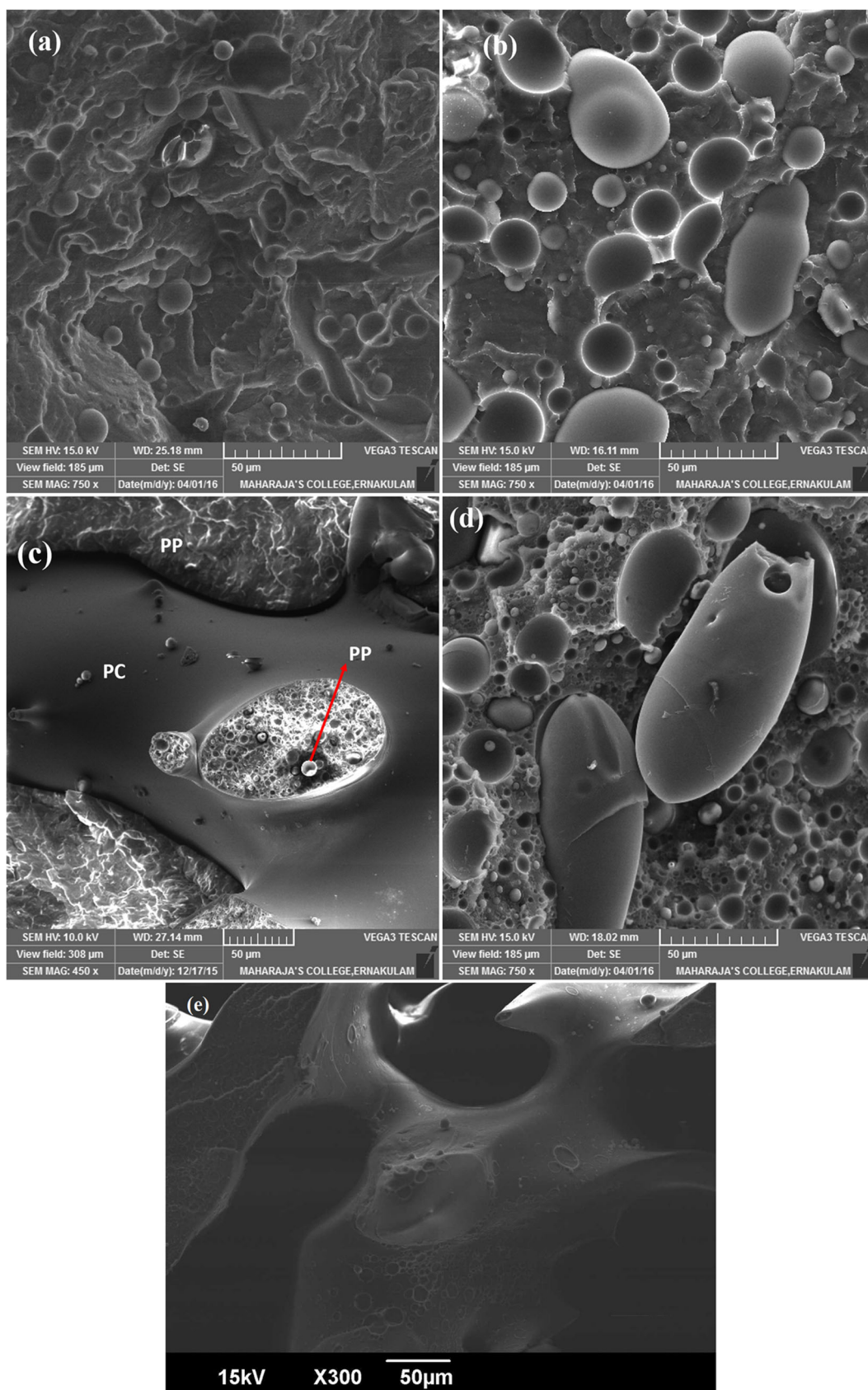


Fig. 1 SEM Images of PC/PP blend (a) PC/PP (10/90); (b) PC/PP (30/70); (c) PC/PP (60/40); (d) PC/PP (70/30); (e) PC phase etched blend PC/PP (60/40)

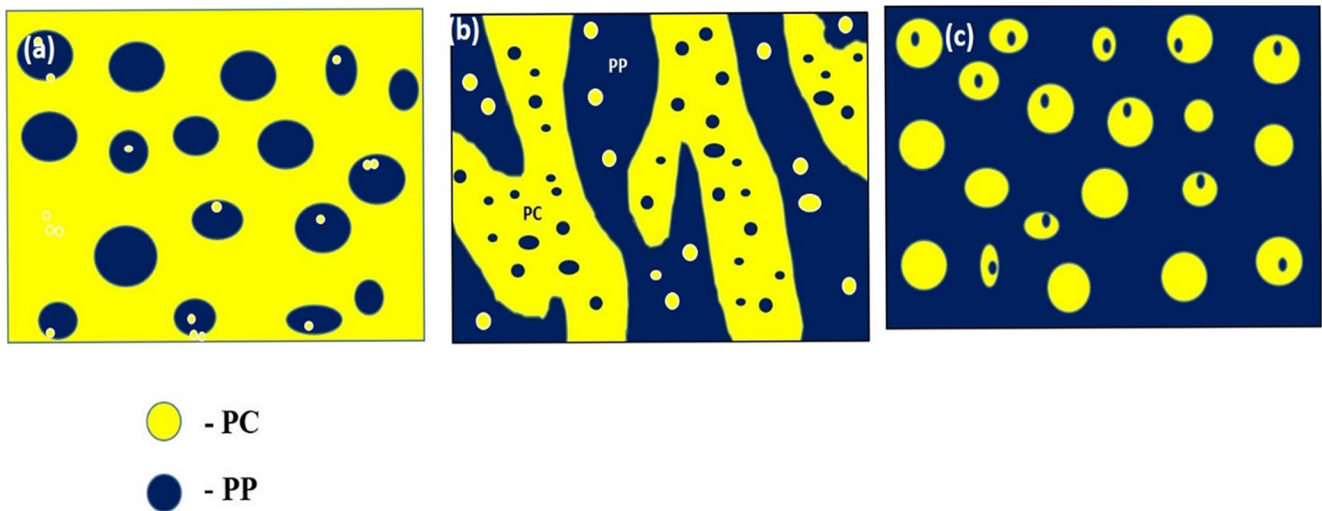


Fig. 2 Schematic representation of viscoelastic phase separation and resulting Phase morphologies of polymer blend system (a) Dispersed morphology (b) Co-continuous (c) Phase inversion, Dispersed phase morphology

The diameter of droplets was determined using *image J* software. Minimum 500 dispersed droplets were considered.

Number-average domain diameter : $D_n = \sum n_i D_i / \sum n_i$ (2)

Weight-average domain diameter : $D_w = \sum n_i D_i^2 / \sum n_i D_i$ (3)

where, n_i and D_i are the numbers and diameter of droplets, respectively. The polydispersity index (PDI) was evaluated based on the ratio of number average diameter and weight average diameter and given as [35].

Polydispersity index : $PDI = D_w / D_n$ (4)

The morphology of polymer blend depends on the viscosity of the component polymers, the compositions and interfacial tension between the polymers. If the two polymers with different viscosities, the microstructure depends on whether the matrix phase has higher or lower viscosity than the minor component. In PC/PP blend system, the polycarbonate has a higher viscosity than polypropylene. The D_n and D_w and PDI values of PC/PP blends are tabulated in Table 1. The number-average domain diameter of dispersed (PC) phase is 9.6 μm

Table 1 The D_n and D_w and PDI values of PC/PP blend composite

Blend Composition	D_n	D_w	PDI
PC/PP(10/90)	9.6 μm	10.5 μm	1.08
PC/PP(20/80)	18.21 μm	22.75 μm	1.23
PC/PP(30/70)	25.19 μm	29.73 μm	1.18
PC/PP(60/40)	Co-continuous system		
PC/PP(70/30)	18.15 μm	21.05 μm	1.12
PC/PP(80/20)	12.8 μm	14.83 μm	1.15

for the PC/PP (10/90) blend and 25.19 μm for the PC/PP (30/70) blend. The D_n and D_w values were found to increase with PC concentration and this is associated with the coalescence of the PC phase. For the PC/PP (60/40) blend, both PC and PP phases form continuous structures. It is very interesting to note that the D_n and D_w values of PC/PP(30/70) blends are higher than PC/PP (70/30) blend system. In PC/PP(70/30) composition, matrix PC phase has higher viscosity than the minor PP phase. The high viscosity PC matrix phase takes up high shear forces and breaks the dispersed PP domains into finer particles. Additionally, due to the high viscosity of the PC phase the diffusional mobility of PP domains is restricted leading to suppression of coalescence, this could be further explained using Wu equation. Wu suggested a simple equation to correlate the domain size with interfacial tension for binary blend [30, 36].

$$d = \frac{4\sigma}{\eta\gamma} \tag{5}$$

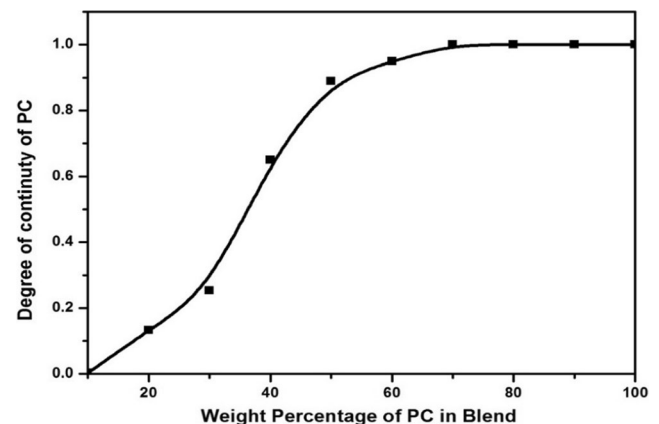


Fig. 3 Degree of continuity of PC with respect to the blend composition

where σ is the interfacial tension, η is the melt viscosity of the matrix phase and γ is the shear rate. From equation no 5, it is clear that the size of droplets is small when the matrix melt viscosity is higher than that of minor component. Thus, when the high viscosity PC is the matrix phase we get small particles of PP droplets.

The co-continuous morphology of the PC/PP (60/40) blends were further confirmed by solvent extraction experiment. Solvent etching test was employed to measure ϕ_i of the PC phase and was calculated using Eq. 1. The degree of continuity (ϕ_i) of the PC phase is presented in Fig. 3. As the amount of PC phase increases, the degree of continuity also increases [4]. At low PC content, the continuity is less, in agreement with the probable morphology of dispersed droplets of the low PC content composition. At 50% PC, the continuity is higher which an indication of more connected morphology. The continuity index approaches 1.0 at 60% of PC in the blend, which confirms that the PC is completely

continuous. For blends having more than 60% PC, sample collapsed during the extraction experiment and continuity could not be measured [37]. This is a clear indication that PP forms a dispersed phase beyond 60 wt% of PC and is in agreement with the morphology data. The curves have been extrapolated to 100% PC with a continuity of index 1.0. A similar behavior was reported by Galloway et al. for POE/PS blends [6].

From solvent extraction studies and SEM studies, we have confirmed that PC/PP (60/40) blend forms co-continuous morphology [38].

Morphology in the presence of MWCNT: Refinement of co-continuous morphology and decrease of the dispersed phase size

Figure 4 illustrates the SEM micrographs of the cryo-fractured blend surface PC/PP (60/40) co-continuous blend with

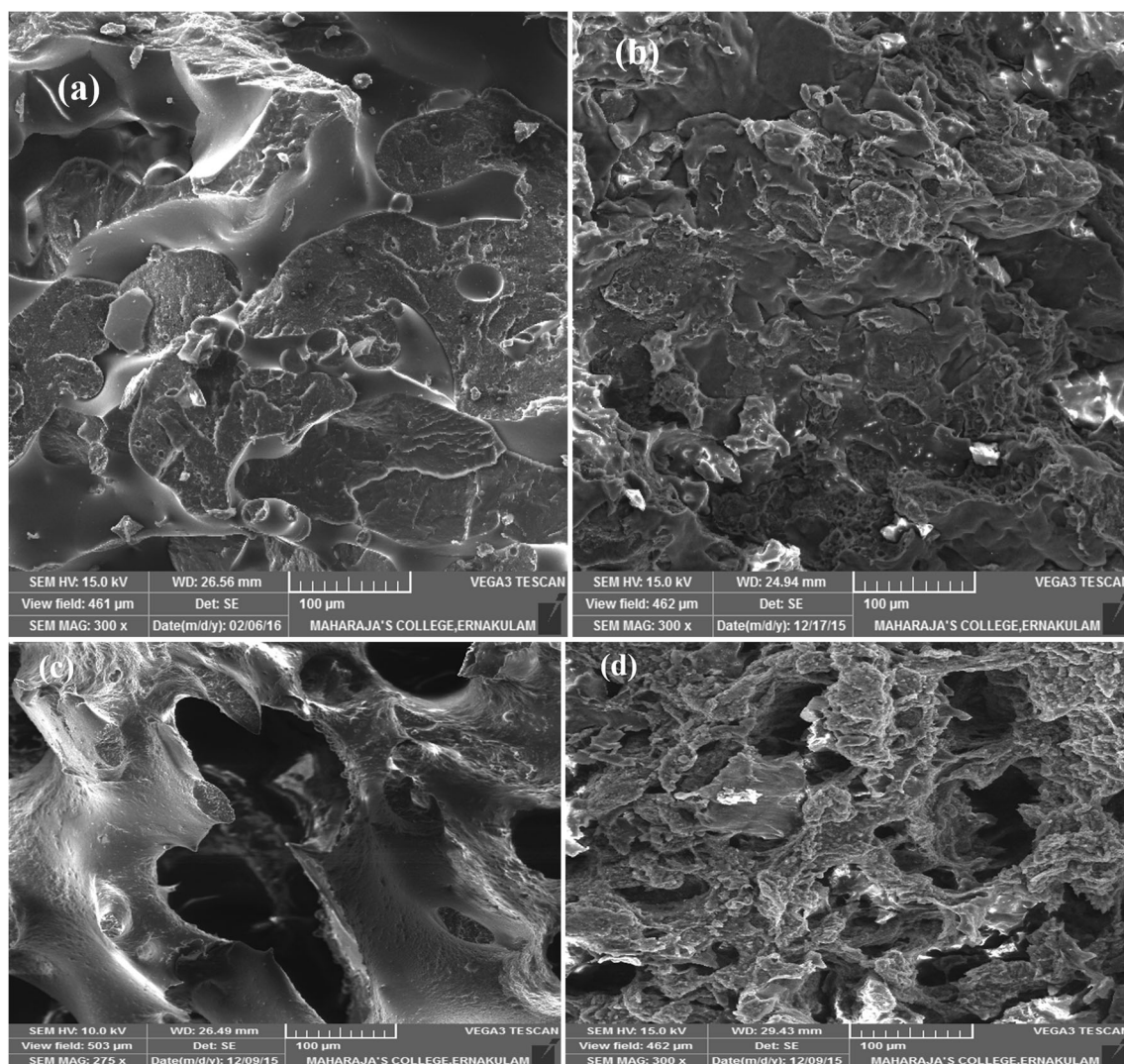


Fig. 4 SEM Images of PC/PP(60/40) blends with (a) 1 wt% MWCNT, (b) 7.5 wt% MWCNT, (c) 1 wt% MWCNT with PC etched surface, (d) 7.5 wt% MWCNT with PC etched surface

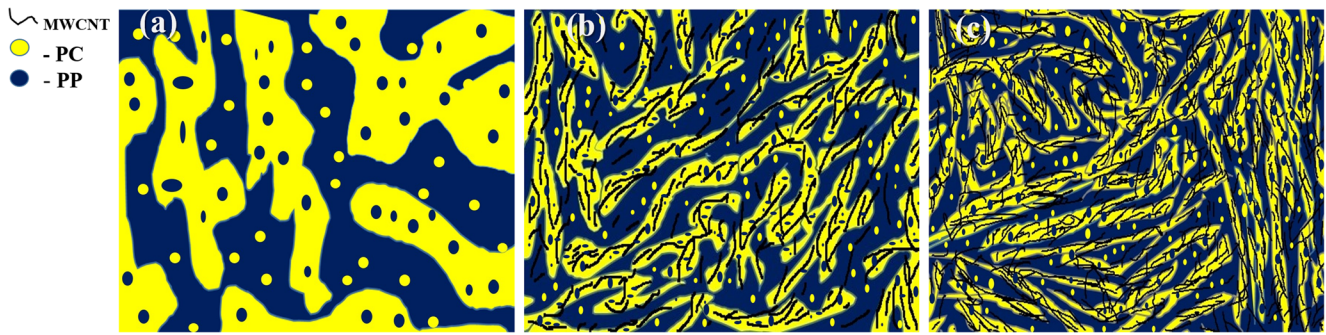


Fig. 5 Schematic representation of refinement of co-continuous phase morphology of PC/PP blend with addition of MWCNTs (a) without MWCNT (b) with low concentration of MWCNT (c) with high concentration MWCNT

MWCNT. To examine the morphology variations as a function of MWCNT content, we have compared the SEM images with different loading of MWCNTs. It is clear that blends with MWCNT also show co-continuous morphology, while a noticeable refinement in the co-continuous microstructure is seen in the blends with MWCNT loading (Fig. 3a-b). Fig. 3c-d show the surfaces PC/PP/MWCNT (60/40) nanocomposites where PC phase was etched out using dichloromethane. From the figures, the blend system showed co-continuous structure in spite of the MWCNT content. The width of the phase structure of both PP and PC phases decreased with the addition of the MWCNT following by a leveling off at higher concentrations of MWCNT.

The refinement of the microstructures of the blends filled with MWCNT can be described by the compatibilizing action of the MWCNTs, which reduces the interfacial tension between the two polymers and suppresses the coalescence. A graphical description of the suggested mechanism is presented in Fig. 5, where the addition of the MWCNT causes

refinement of the co-continuous morphology [39]. Figure 6 shows the degree of continuity of the PC phase versus MWCNT loading for PC/PP (60/40) blends as determined from quantitative solvent extraction experiment. As the MWCNT loading increases, the degree of continuity of PC remains unaffected. It indicates that the co-continuous morphology of PC/PP (60/40) has been unchanged by the inclusion of MWCNT [40]. However, as indicated earlier, it is very interesting to note that the average phase thickness of the PP and PC phase is found to decrease with the addition of MWCNT followed by leveling off at higher concentrations. It has been quantified. The average phase thickness vs. MWCNT loading is plotted as shown in Fig. 7. The Fig. 7 clearly indicates that both PP and PC phases interpenetrate very efficiently in the presence of MWCNTs.

The influence of MWCNT on the dispersed phase (sea-island) morphology also studied. As a representative model, we have examined the morphology of PC/

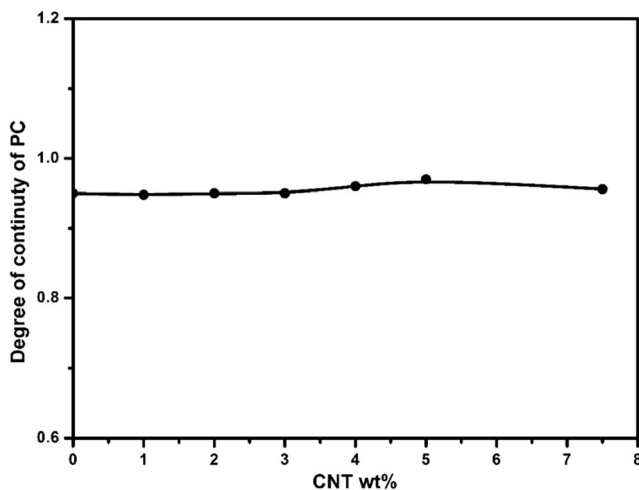


Fig. 6 Degree of continuity (θ_i) of PC with respect to the MWCNT loading for PC/PP (60/40)/MWCNT blend

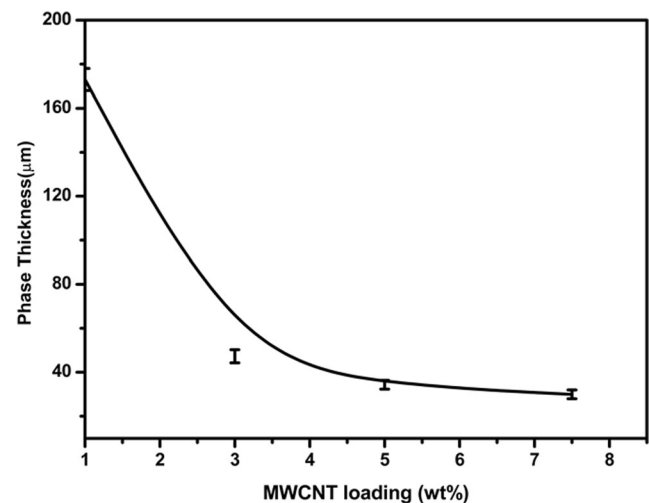


Fig. 7 Graph showing the variation of average phase thickness of PC/PP (60/40) vs. MWCNT loading (wt%)

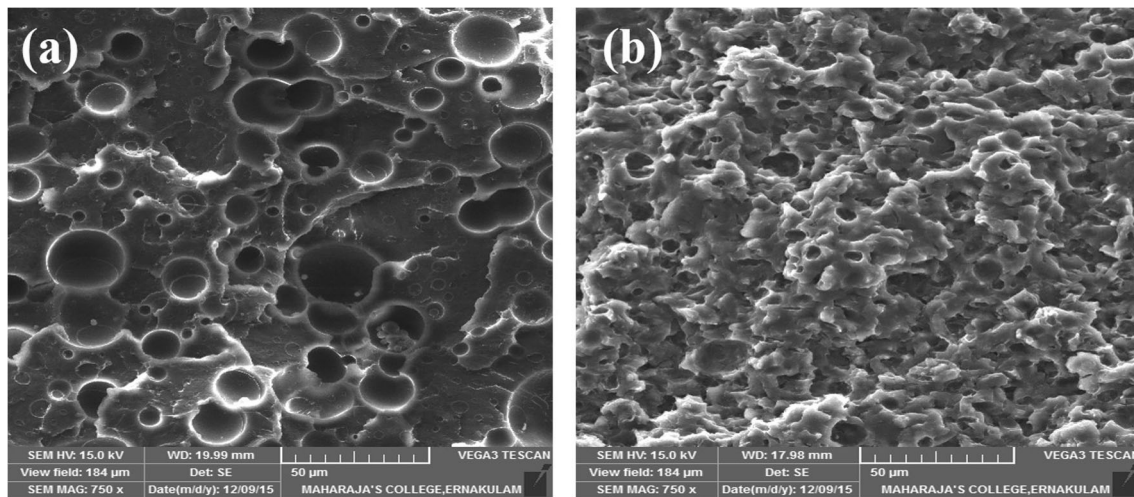


Fig. 8 SEM Image of PC phase etched PC/PP(20/80) blend composite (a) without MWCNT (b) with 5 wt% of MWCNT

PP (20/80) blend as a function of MWCNT content. In this blend composition, PC forms the dispersed phase in the continuous PP matrix. It can be seen that the diameter of the PC droplets is decreased with the addition of MWCNT into the blend system, as shown in Fig. 8. The average diameter of PC droplets reduced from 18.2 μm to 7.2 μm with the addition of 5 wt% of MWCNT into the blend followed by a leveling off as shown in Fig. 9. The remarkable change in the size reduction indicated that MWCNT plays a major role in compatibilising of immiscible PP/PC blends [41–44]. The observed compatibilising action could be explained as being due to: 1) the suppression of coalescence of the dispersed phase by the MWCNTs which act as a physical barrier against particle/particle agglomeration; 2) the decrease of interfacial tension by the localisation

of the MWCNT at the blend interface. The behaviour is analogous to the action of block and graft copolymers in incompatible polymer/polymer blends where the compatibilising action is associated with the suppression of coalescence and interfacial tension reduction. A similar phenomenon was reported by Liu et al. for PA6/ABS/MWCNT nanocomposites [44].

Localisation of MWCNTs in the blend: Thermodynamic considerations

We can calculate thermodynamically the preferred MWCNTs position from wetting coefficient ω_a [22, 45]. The wetting coefficient (ω_a) can be calculated using Young's equation.

$$\omega_a = \frac{\gamma_{CNT-PC} - \gamma_{CNT-PP}}{\gamma_{PP-PC}} \quad (6)$$

where γ_{CNT-PC} , γ_{CNT-PP} and γ_{PP-PC} are the interfacial energies between the PC and MWCNTs, the PP and MWCNTs respectively. If the wetting coefficient is greater than 1, preferred phase of MWCNT is polypropylene phase and if ω_a is less than -1 , preferred phase of MWCNT is polycarbonate (PC). If ω_a is between -1 and 1, then MWCNT will be at the interface. Surface energies of PC and PP at 230 $^{\circ}\text{C}$ were calculated using eq. 7 and 8 and with respect to the surface energies of the sample at 20 $^{\circ}\text{C}$ [46] which are detailed in Tables 2 and 3.

$$-d\gamma/dT = (11/9)(\gamma_0/T_c)(1-T/T_c)^{2/9} \quad (7)$$

$$\gamma = \gamma_0(1-T/T_c)^{11/9} \quad (8)$$

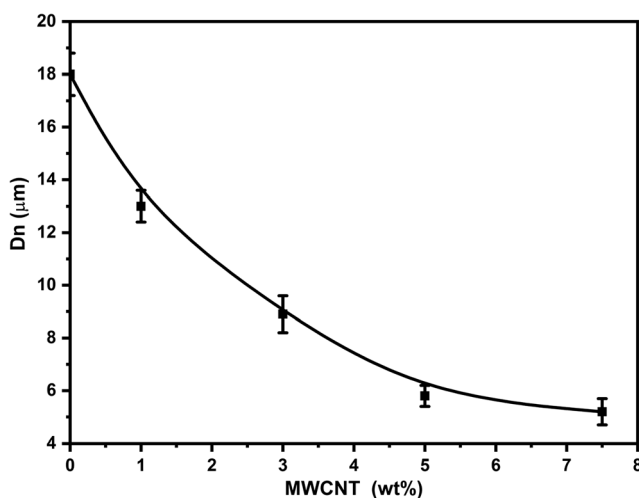


Fig. 9 Variation of Dn Vs MWCNT loading

Table 2 Surface energy of MWCNTs, PC, and PP at 20 °C

Material	Dispersive Component (mJ.m ⁻²)	Polar Component (mJ.m ⁻²)	Total (mJ.m ⁻²)
PC	27.7	6.5	34.2
PP	30.1	0	30.1
MWCNTs	17.6	10.2 [45]	27.8

where γ_0 is the surface energies at 0 K, T is the temperature and T_c is the critical temperature and $T_c \sim 1000$ K. The wetting characteristics of MWCNTs have been previously reported [22, 47, 48]. The MWCNTs used in this work are non-functionalized. In fact, we have calculated the surface energies of MWCNTs based on assumptions of Barber et al. [48].

The surface energies of PC, PP and MWCNTs at 230 °C are tabulated in Table 3. The interfacial tension can be evaluated from the surface energies and their dispersive and polar components. Both the harmonic mean equation (Eq. 9) and geometric mean equation (Eq. 10) were used to evaluate the interfacial energies.

$$\gamma_{12} = \gamma_1 + \gamma_2 - 4 \left[\frac{\gamma_1^d \gamma_2^d}{\gamma_1^d + \gamma_2^d} + \frac{\gamma_1^p \gamma_2^p}{\gamma_1^p + \gamma_2^p} \right] \quad (9)$$

$$\gamma_{12} = \gamma_1 + \gamma_2 - 2 \left(\sqrt{\gamma_1^d \gamma_2^d} + \sqrt{\gamma_1^p \gamma_2^p} \right) \quad (10)$$

Where γ_1 and γ_2 , are the surface free energies, γ_1^d and γ_2^d are the dispersion components of the surface energies of first and second blend components. γ_1^p and γ_2^p are the polar components of the surface energies of polymer component 1 and 2 respectively.

The estimated interfacial energies using eq. 9 and 10 are presented in Table 4. The calculated wetting coefficient (ω_a) according to equations no. 9 and 10 are -1.3 and -1.4, respectively. The ω_a for composite is < -1, therefore the thermodynamically preferred phase of MWCNTs is the PC phases.

We have examined the phase morphology and MWCNT dispersion of PC/PP (60/40) blends by high resolution electron microscopy (SEM and TEM). Fig. 10 a and b very clearly indicates that the PC/PP (60/40) system in presence of MWCNT shows the co-continuous structure in agreement with our solvent extraction data. Additionally, the high-resolution SEM data (Fig. 10) indicates that the wall thickness of both continuous PC and PP decreases with MWCNT loading as indicated by brown lines. As shown in Fig. 10 the MWCNTs are preferentially localized at PC phase (as indicated by yellow circle). The selective localisation of MWCNTs in the PC phase could be due to the polarity of PC phase and thermodynamic affinity of MWCNTs towards the PC phase. We can also notice that small quantity of the MWCNTs is localised at the blend interface and PP phase (as indicated by green circle and red arrows). The blend system with MWCNT showed strong viscoelastic phase separation process as indicated by the phase in phase morphology. In fact, since the majority of the MWCNT is located at the PC phase, its viscosity must have gone up and this must have accelerated the viscoelastic phase separation process as the viscosity disparity between the phases (PC and PP) increased.

Figure 11 shows high-resolution TEM micrographs of PC/PP(60/40) with 3 and 5 wt% of MWCNT. In the TEM micrograph, PP phases appear as white regions whereas PC phase appears as dark regions [49, 50]. The SEM and TEM data were complimentary to each other. Large number of MWCNTs can be seen dispersed at the PC phase of the PC/PP/MWCNT 3 wt% blend, and a small amount of MWCNTs is localised at the

Table 3 Surface energy of MWCNTs, PC and PP at 230 °C

Material	Dispersive Component (mJ.m ⁻²)	Polar Component (mJ.m ⁻²)	Total (mJ.m ⁻²)
PC	17.9	4.2	22.2
PP	17.7	0	17.7
MWCNTs	11.4	6.6	18

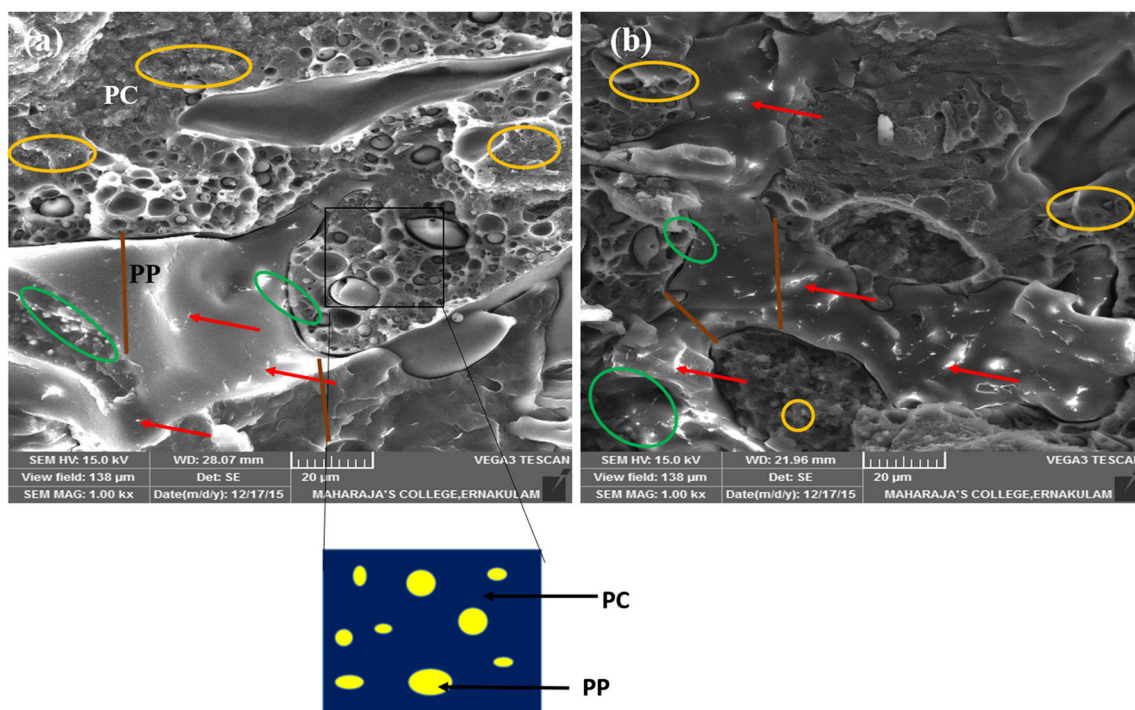
Table 4 Interfacial energies as evaluated using Eq. 9 and 10

Material	Based on harmonic mean equation ($\text{mJ}\cdot\text{m}^{-2}$)	Based on geometric mean equation ($\text{mJ}\cdot\text{m}^{-2}$)
PC/PP	3.9	4.2
PC/MWCNTs	-3.4	-3.7
PP/MWCNTs	2.4	2.5

interface (marked as red circle) and in the PP phase also. The TEM images of the PC/PP (60/40)/MWCNT 5 wt% blend is shown in Fig. 10 b. In this case also, number of the MWCNTs are distributed in the PC phase and a lesser number of the MWCNTs were distributed at the interface and PP phase. This result strongly indicates that the MWCNTs moves to the boundary as the viscosity of the PC phase increases [51]. Localisation of MWCNTs also depends upon the viscosities and affinity between the components. Many researchers have been reported that fillers choose to be confined in the polymer component with low viscosity [51, 52]. If the viscosity mismatch of two polymers is small, nanofillers will be confined in the component with higher thermodynamic affinity. As the viscosity of the PC component is higher than the PP phase, MWCNTs will have the tendency to go to PP phase. However, since PC is polar, PC is the favoured phase thermodynamically. There exist a competition between thermodynamics and kinetics factors. However, experimental observations

indicated that MWCNTs are more localised in the PC phase forming percolating network dominating the thermodynamic effect. However, we could see, minor amount of MWCNTs in the PP and interface.

To better understand the localisation of MWCNT in the blend, the experiments were performed where the MWCNT was first melt mixed with one polymer and then the resulting composite was mixed with the second polymer. The MWCNTs were even found to be in both phases and interface when they were pre-dispersed in PC (or PP) before subsequent melt blend with neat PP (or PC). Here, the MWCNTs were found to be migrating from pre-dispersed phase to neat phase during the melt mixing. The Fig. 12.a shows the TEM image of the nanocomposite, the MWCNTs were pre-dispersed with PC phase and subsequently melt mixed with neat PP. From the TEM image, it's clear that MWCNTs are migrated from PC phase to neat PP phase. The red arrows indicated that MWCNTs are migrating from PC (premixed phase) phase to PP phase. Here the kinetic factor is playing a major role in the distribution of MWCNTs. In the case, where MWCNTs were

**Fig. 10** SEM micrographs of (a) PC/PP (60/40)/MWCNT3wt%; (b) PC/PP (60/40)/MWCNT 5 wt%

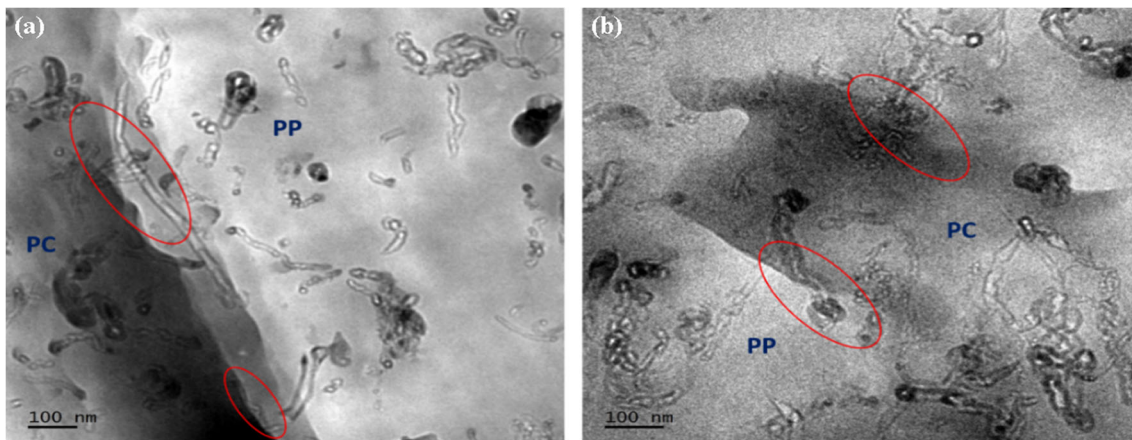


Fig. 11 TEM images of (a) PC/PP (60/40)/MWCNT 3 wt%;(b) PC/PP (60/40)/MWCNT 5 wt%

pre-dispersed with PP and subsequently melt mixed with neat PC, the MWCNTs are migrated from pre-dispersed phase to PC phase (Fig. 12.b). In the Fig. 12.b, the red arrows indicated that MWCNTs are migrating from PP (premixed phase) phase to PC phase. It is due to the thermodynamic affinity of MWCNTs towards the PC phase. There exist a competition between thermodynamics and kinetics factors. Hence, the distribution of MWCNTs in PC/PP composite is really a compromise of these two factors [24, 53, 54]. In fact the interfacial localisation of MWCNT plays a major role of compatibilisation of the blends and viscoelastic phase separation process.

Viscoelastic properties

Figure 13 illustrates the storage modulus of PC, PP and PC/PP (60/40) blends as a function of frequency which varies from 0.1 to 100 rad/s. The modulus of the PC phase is found to be higher than the PP phase over the entire frequency range. The modulus of the

blend is intermediate to the component polymers, however, the behaviour is not strictly composition dependent on the high-frequency region whereas the blend behaviour is more towards the PP phase. As discussed earlier, the PC/PP (60/40) blend system has a co-continuous morphology where both phases interpenetrate each other and the modulus displays power law characteristics at low-frequency region [55]. At low frequency, the slope of the PC/PP (60/40) blend curve is smaller than constituent polymers. This may be described by the co-continuous microstructure of blend system. The behaviour is characterised by $G' \propto \omega^\alpha$ with $\alpha < 1$. The domains with different lengths scale produce relaxation processes with different characteristics times [55, 56]. Fig. 14 shows the Cole- Cole plot that in fact defines the connection between η'' ($\eta'' = G''/\omega$) and η' ($\eta' = G'/\omega$) and relates to the relaxation spectrum of chain orientation. A tail appears at high values, which corresponds to the relaxation of networks of co-

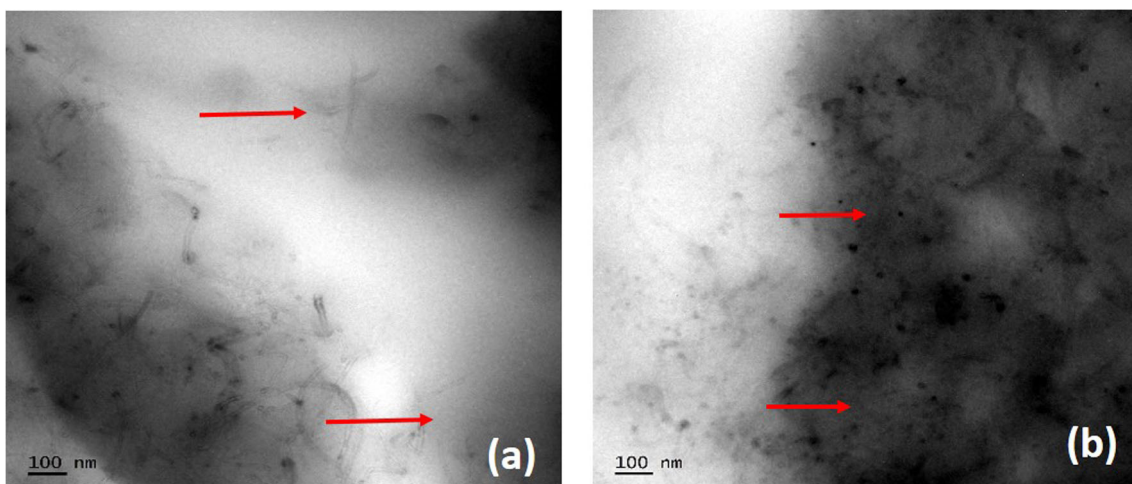


Fig. 12 TEM images of (a) PC-MWCNT (3 wt%)/PP; (b) PC/PP-MWCNT (3 wt%)

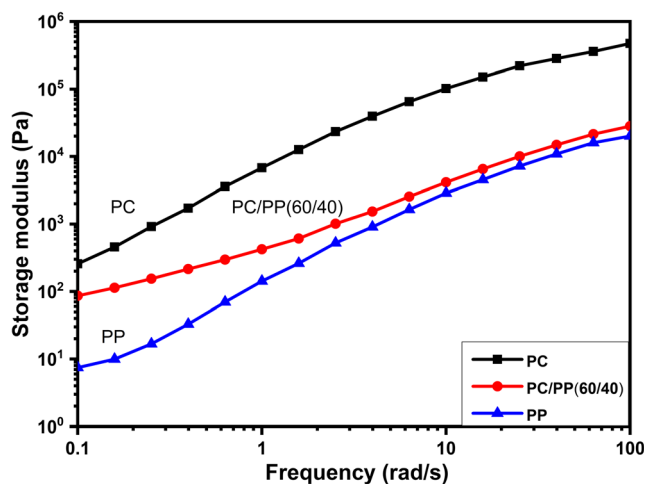


Fig. 13 Storage modulus $G'(\omega)$ as a function of frequency for PP, PC and PC/PP(60/40) blend

continuous phases. These properties are manifestation of the power law characteristics in the low-frequency region [57, 58].

Rheological analysis based on oscillatory shear could be used for predicting blends structure-property correlations. The linear viscoelastic response of the PC/PP blend were investigated by performing SAOS (small amplitude oscillatory shear) test. Storage modulus of the blends from SAOS analysis are shown in Fig. 15. From figure it can be seen, the slope of the modulus decrease with respect to the phase morphology (from droplets to co-continuous morphology) of the blends. For co-continuous blend (60/40) modulus value are nearly frequency independent in the low frequency zone, which is indicative of the formation of interconnected morphology of PC and PP in the blend [59, 60].

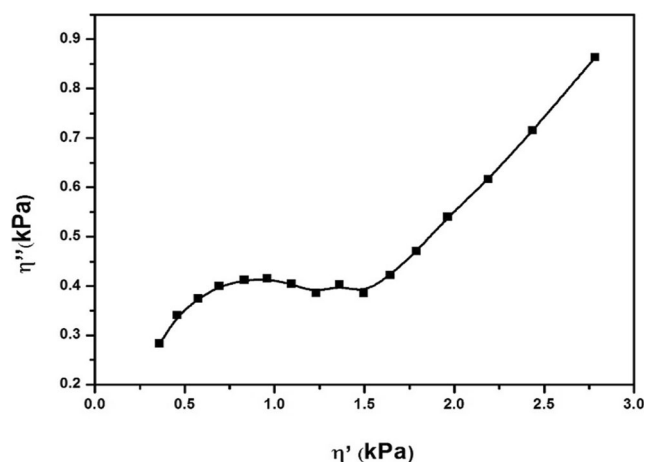


Fig. 14 Cole-Cole plots of the PC/PP (60/40) blend

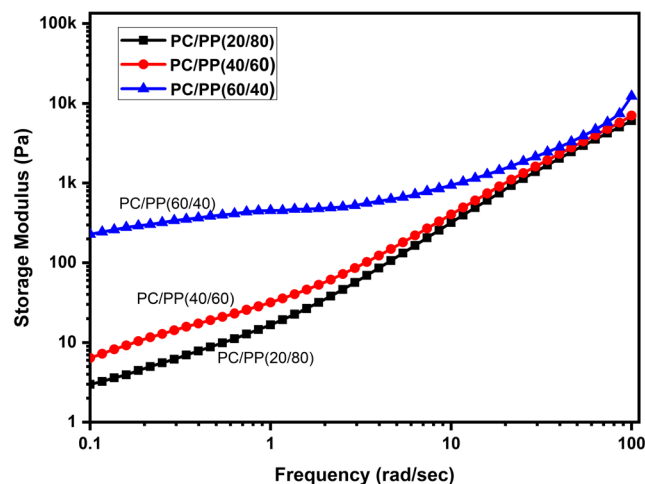


Fig. 15 Storage modulus of the PC/PP blends from SAOS analysis

The viscoelastic properties of the blend /MWCNT nanocomposites are presented in Fig. 16. Due to the selective localisation of the MWCNTs in the PC phase, the phase morphology is highly refined. The interfacial localisation of MWCNTs gives rise to a percolating network structure in the polymer blend resulting in a stable and homogenous morphology. M. Moniruzaman and K.I. Winey was discussed in detail the rheological behaviour of CNT contained polymer nanocomposites [61]. The rheological response can serve as a qualitative measure of the dispersion state of the fillers in the composites. As the MWCNT loading is increased, storage modulus (G') also increases (Fig. 16.a). At 1 wt% MWCNT loading, no reinforcing effect was seen compared to higher filler loading because, at very low nanotube loading, it acts as a flaw in the blend matrix [62]. At low-frequency region, the non-terminal behaviour in the storage modulus and viscosity upturn are more pronounced with MWCNT content. It means that, the rheological behavior progress from a liquid like response ($G' \propto \omega^2$) to a solid like response (G' independent of ω) with MWCNT loading. At low frequency, the storage modulus is increases and the slope of curve is decreases with nanotube concentration. This is because the polymer chain relaxations effectively restrained by the nanotubes due to the better dispersion in the composites. A similar phenomenon was reported by Amir et al. [63] for PC/ABS/MWCNT nanocomposites. At high-frequency region, the effect of the MWCNT addition on the storage modulus and viscosity is relatively weak. It means that MWCNTs does not significantly influence the short-range motion of polymer chains and also due to the high relaxation time of polymer chain at high

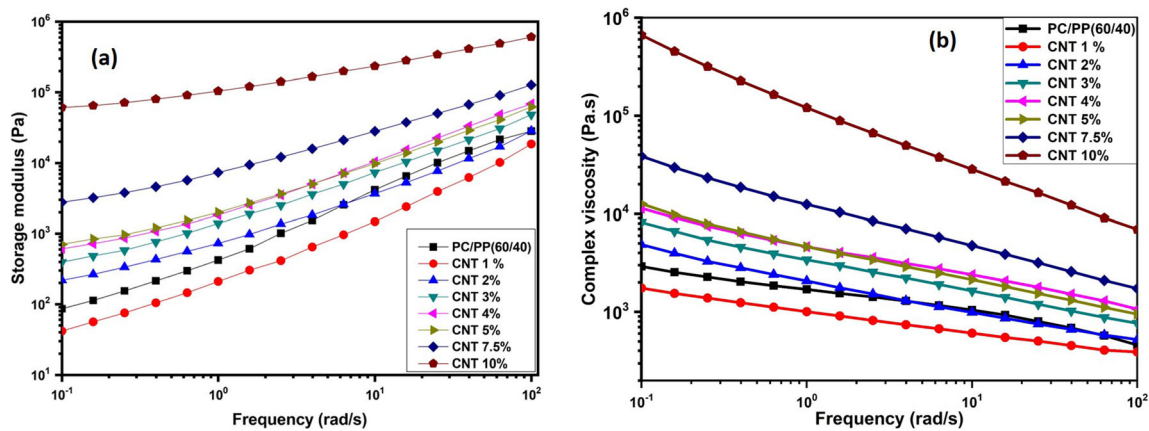


Fig. 16 (a) Storage modulus for PC/PP (60/40)/MWCNT nanocomposites (b) Complex viscosity for MWCNT filled PC/PP (60/40)

frequencies [61]. As observed in the complex viscosity graphs, the samples show shear thinning behaviour with frequency, indicating pseudoplastic behaviour (Fig. 16.b). The slope of the complex viscosity is increased with MWCNT. This is due to the orientation of MWCNT at high shear rates.

The rheological percolation of the nanocomposites was calculated from Van Gorp Palmen Plots. The phase angle (δ°) is drawn against complex modulus (G^*) and shown in Fig. 17.

The phase angle slope varies from negative to positive along with complex modulus. It may be due to the enhancement of the elasticity of composite by MWCNT network [64]. A substantial change in slope of the curve is seen at above 5 wt% of MWCNT and below this, the phase angle curve approaches to an angle near 70° indicating the dominating viscous flow behaviour. As the MWCNTs loading is increased to 5 wt%, the lower frequency phase angle decreases to less than 55° representing a rheological viscous fluid - solid evolution. Beyond 7.5 wt% MWCNT loading, the lower

frequency phase angle dramatically decreases, indicating a very strong solid-like behaviour. From Fig. 16, it is very clear that the system shows percolation process at 5 wt% of MWCNT. This behaviour is indicative of a rheological percolation at which the nanotubes delayed the motion of polymer chains.

Conclusions

In this study, we have studied the effect of the addition of multiwalled carbon nanotube on morphology and viscoelastic properties of PC/PP blend nanocomposites. The SEM and solvent extraction studies confirmed that PC/PP (60/40) blend has co-continuous morphology. Both the neat blends and blend nanocomposites showed viscoelastic phase separation due to viscosity difference and T_g differences of polymers (PP and PC). We could observe phase in phase morphology. A substantial refinement in the co-continuous structure was also observed with the addition of MWCNT. The size of the dispersed PC droplet was found to decrease with the addition of the MWCNT followed by a levelling off at higher concentration. This behaviour is analogous to the action of block copolymers in polymer/polymer blends. The significant change in the phase thickness and droplets size indicated that MWCNT plays a major role in compatibilising immiscible PP/PC blends. Theoretical predictions based on thermodynamic considerations clearly indicated the preferential localisation of MWCNTs in the PC phase. As a result the viscoelastic phase separation became more predominant due to the increase in viscosity of the PC phase. Due to the viscosity differences between the two polymers, we found that some of the MWCNTs are localised at the blend interphase and in PP phase as being evidenced by the high resolution TEM data. The storage modulus and complex viscosity of blend nanocomposites were increased with the addition of MWCNTs. At low frequency region, non-terminal characteristics, viscosity

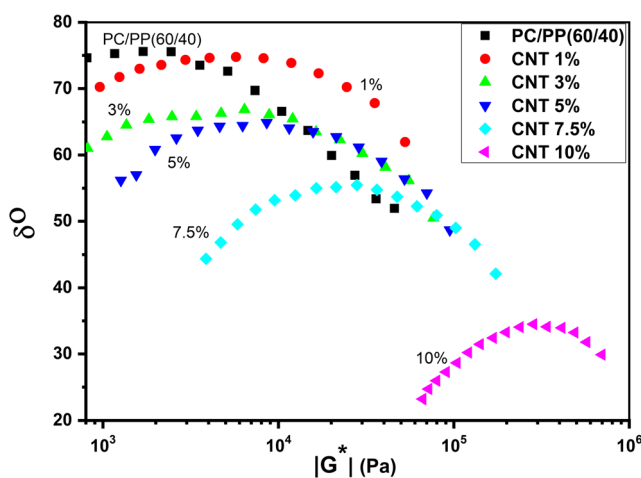


Fig. 17 Van GorpPalmen Plot for PC/PP (60/40)/MWCNT nanocomposites

uptum were observed, indicating a 3D network formation of MWNCTs in the polymer matrix. The rheological percolation threshold was determined from storage modulus curves and Van Gurp Palmén Plot. The nanocomposite system showed percolation process at 5 wt% of CNT loading.

Acknowledgments This project is funded by Ministry of Electronics and Information Technology-MeitY (F. No. 1(2)/2012-EMCD), Govt. of India, New Delhi. The authors also would like to acknowledge the financial support from DST-Nanomission – Govt. of India and UGC – Govt. of India.

Compliance with ethical standards

Conflict of interest There are no conflicts of interest to declare.

References

- Utracki LA (1982) Economics of polymer blends. *Polym Eng Sci* 22:1166–1175
- Utracki LA (1999) Polymer blends: fundamentals. Polypropylene, Polymer Sc. Springer, pp 601–605
- Paul DR, Barlow JW (1980) Polymer blends. *J Macromol Sci Macromol Chem* 18:109–168
- Machado JM, Lee CS (1994) Compatibilization of immiscible blends with a mutually miscible third polymer. *Polym Eng Sci* 34:59–68
- Uemura T, Kaseda T, Sasaki Y, Inukai M, Toriyama T, Takahara A, Jinnai H, Kitagawa S (2015) Mixing of immiscible polymers using nanoporous coordination templates. *Nat Commun* 6:7473
- Galloway JA, Koester KJ, Paasch BJ, Macosko CW (2004) Effect of sample size on solvent extraction for detecting cocontinuity in polymer blends. *Polymer* 45:423–428
- Castro M, Carrot C, Prochazka F (2004) Experimental and theoretical description of low frequency viscoelastic behaviour in immiscible polymer blends. *Polymer* 45:4095–4104
- Huang S, Bai L, Trifkovic M, Cheng X, Macosko CW (2016) Controlling the morphology of immiscible cocontinuous polymer blends via silica nanoparticles jammed at the interface. *Macromolecules* 49:3911–3918
- Altobelli R, de Luna MS, Causa A et al (2016) Morphology stabilization of co-continuous polymer blends through clay nanoparticles. AIP conference proceedings. AIP Publishing, 20057
- Li L, Miesch C, Sudeep PK, Balazs AC, Emrick T, Russell TP, Hayward RC (2011) Kinetically trapped co-continuous polymer morphologies through intraphase gelation of nanoparticles. *Nano Lett* 11:1997–2003
- Popov VN (2004) Carbon nanotubes: properties and application. *Mater Sci Eng R Reports* 43:61–102
- Iijima S (1991) Helical microtubules of graphitic carbon. *Nature* 354:56–58
- Tao F, Auhl D, Baudouin A et al (2013) Influence of multiwall carbon nanotubes trapped at the interface of an immiscible polymer blend on interfacial tension. *Macromol Chem Phys* 214:350–360
- Mamunya Y, Levchenko V, Boiteux G, Seytre G, Zanoaga M, Tanasa F, Lebedev E (2016) Controlling morphology, electrical, and mechanical properties of polymer blends by heterogeneous distribution of carbon nanotubes. *Polym Compos* 37:2467–2477
- Pradhan B, Setyowati K, Liu H, Waldeck DH, Chen J (2008) Carbon nanotube–polymer nanocomposite infrared sensor. *Nano Lett* 8:1142–1146
- Njuguna J, Pielichowski K (2003) Polymer nanocomposites for aerospace applications: properties. *Adv Eng Mater* 5:769–778
- Singh BP, Saini P, Gupta T et al (2011) Designing of multiwalled carbon nanotubes reinforced low density polyethylene nanocomposites for suppression of electromagnetic radiation. *J Nanopart Res* 13:7065–7074
- Poathanari MA, Abraham J, Kalarikkal N, Thomas S (2018) Excellent electromagnetic interference shielding and high electrical conductivity of Compatibilized polycarbonate/polypropylene carbon nanotube blend nanocomposites. *Ind Eng Chem Res* 57:4287–4297
- Botelho EC, Costa ML, Braga CI, Burkhart T, Lauke B (2013) Viscoelastic behavior of multiwalled carbon nanotubes into phenolic resin. *Mater Res* 16:713–720
- Cassagnau P (2013) Linear viscoelasticity and dynamics of suspensions and molten polymers filled with nanoparticles of different aspect ratios. *Polymer* 54:4762–4775
- Pötschke P, Pegel S, Claes M, Bonduel D (2008) A novel strategy to incorporate carbon nanotubes into thermoplastic matrices. *Macromol Rapid Commun* 29:244–251
- Koysuren O, Yesil S, Bayram G (2010) Effect of solid state grinding on properties of PP/PET blends and their composites with carbon nanotubes. *J Appl Polym Sci* 118:3041–3048
- Liebscher M, Tzounis L, Pötschke P, Heinrich G (2013) Influence of the viscosity ratio in PC/SAN blends filled with MWCNTs on the morphological, electrical, and melt rheological properties. *Polymer* 54:6801–6808
- Wu D, Zhang Y, Zhang M, Yu W (2009) Selective localization of multiwalled carbon nanotubes in poly(epsilon-caprolactone)/polylactide blend. *Biomacromolecules* 10:417–424
- Cardinaud R, McNally T (2013) Localization of MWCNTs in PET/LDPE blends. *Eur Polym J* 49:1287–1297
- Abbasi Moud A, Javadi A, Nazockdast H, Fathi A, Altstaedt V (2015) Effect of dispersion and selective localization of carbon nanotubes on rheology and electrical conductivity of polyamide 6 (PA6), polypropylene (PP), and PA6/PP nanocomposites. *J Polym Sci Part B Polym Phys* 53:368–378
- Du F, Scogna RC, Zhou W et al (2004) Nanotube networks in polymer nanocomposites: rheology and electrical conductivity. *Macromolecules* 37:9048–9055
- Mohammed Arif P, Sarathchandran C, Narayanan A, Saiter A, Terzano R, Allegretta I, Porfido C, Kalarikkal N, Thomas S (2017) Multiwalled carbon nanotube promotes crystallisation while preserving co-continuous phase morphology of polycarbonate/polypropylene blend. *Polym Test* 64:1–11
- Favis B, Chalifoux J (1988) Influence of composition on the morphology of polypropylene/polycarbonate blends. *Polymer* 29:1761–1767
- Zhihui Y, Yajie Z, Xiaomin Z, Jinghua Y (1998) Effects of the compatibilizer PP-g-GMA on morphology and mechanical properties of PP/PC blends. *Polymer* 39:547–551
- Xu Y, Sun Z, Chen X, Chen M, Hu S, Zhang Z (2013) Mechanical properties and crystallization behavior of polycarbonate/polypropylene blends. *J Macromol Sci Part B* 52:716–725
- Babu RR, Singha NK, Naskar K (2011) Phase morphology and melt rheological behavior of uncrosslinked and dynamically crosslinked polyolefin blends: role of macromolecular structure. *Polym Bull* 66:95–118
- Shi W, Chen F, Zhang Y, Han CC (2012) Viscoelastic phase separation and interface assisted crystallization in a highly immiscible iPP/PMMA blend. *ACS Macro Lett* 1:1086–1089

34. Paukszta D, Garbarczyk J, Sterzyński T (1995) Structure of polypropylene/polycarbonate blends crystallized under pressure. *Polymer* 36:1309–1313
35. Chandran N, Chandran S, Maria HJ, Thomas S (2015) Compatibilizing action and localization of clay in a polypropylene/natural rubber (PP/NR) blend. *RSC Adv* 5:86265–86273
36. Wu S (1987) Formation of dispersed phase in incompatible polymer blends: interfacial and rheological effects. *Polym Eng Sci* 27:335–343
37. Galloway JA, Macosko CW (2004) Comparison of methods for the detection of cocontinuity in poly (ethylene oxide)/polystyrene blends. *Polym Eng Sci* 44:714–727
38. Li C, Tian G, Zhang Y, Zhang Y (2002) Crystallization behavior of polypropylene/polycarbonate blends. *Polym Test* 21:919–926
39. Filippone G, Dintcheva NT, La Mantia FP, Aciemo D (2010) Using organoclay to promote morphology refinement and co-continuity in high-density polyethylene/polyamide 6 blends—effect of filler content and polymer matrix composition. *Polymer* 51:3956–3965
40. Bose S, Bhattacharyya AR, Khare RA, Kulkarni AR, Umasankar Patro T, Sivaraman P (2008) Tuning the dispersion of multiwall carbon nanotubes in co-continuous polymer blends: a generic approach. *Nanotechnology* 19:335704
41. Parpaite T, Otazaghine B, Taguet A, Sonnier R, Caro AS, Lopez-Cuesta JM (2014) Incorporation of modified Stöber silica nanoparticles in polystyrene/polyamide-6 blends: coalescence inhibition and modification of the thermal degradation via controlled dispersion at the interface. *Polymer* 55:2704–2715
42. Chow WS, Ishak ZA (2015) Polyamide blend-based nanocomposites: a review. *Express Polym Lett* 9:211–232
43. Zhang L, Wan C, Zhang Y (2009) Morphology and electrical properties of polyamide 6/polypropylene/multi-walled carbon nanotubes composites. *Compos Sci Technol* 69:2212–2217
44. Liu X-Q, Yang W, Xie B-H, Yang M-B (2012) Influence of multi-wall carbon nanotubes on the morphology, melting, crystallization and mechanical properties of polyamide 6/acrylonitrile–butadiene–styrene blends. *Mater Des* 34:355–362
45. Zhou J, Min BG (2013) Interfacial localization of multiwalled carbon nanotubes in immiscible blend of poly (ethylene terephthalate)/polyamide 6. *Fibers Polym* 14:518–524
46. Solid surface energy data (SFE) for common polymers. In: <http://www.surface-tension.de/solid-surface-energy.htm> (Accessed: 25.02.2016)
47. Nuriel S, Liu L, Barber AH, Wagner HD (2005) Direct measurement of multiwall nanotube surface tension. *Chem Phys Lett* 404:263–266
48. Barber AH, Cohen SR, Wagner HD (2004) Static and dynamic wetting measurements of single carbon nanotubes. *Phys Rev Lett* 92:186103
49. Nair ST, Vijayan PP, Xavier P et al (2015) Selective localisation of multi walled carbon nanotubes in polypropylene/natural rubber blends to reduce the percolation threshold. *Compos Sci Technol* 116:9–17
50. Favis BD, Le Corroller P Polymeric material and process for recycling plastic blends. US 9,670,344
51. Feng J, Chan C, Li J (2003) A method to control the dispersion of carbon black in an immiscible polymer blend. *Polym Eng Sci* 43:1058–1063
52. Guo C, Zhou L, Lv J (2013) Effects of expandable graphite and modified ammonium polyphosphate on the flame-retardant and mechanical properties of wood flour–polypropylene composites. *Polym Polym Compos* 21:449–456
53. Vo L, Giannelis E (2007) Compatibilizing poly (vinylidene fluoride)/nylon-6 blends with nanoclay. *Macromolecules* 40:8271–8276
54. Zhao X, Zhao J, Cao J-P, Wang X, Chen M, Dang ZM (2013) Tuning the dielectric properties of polystyrene/poly (vinylidene fluoride) blends by selectively localizing carbon black nanoparticles. *J Phys Chem B* 117:2505–2515
55. Weis C, Leukel J, Borckenstein K, Maier D, Gronski W, Friedrich C, Honerkamp J (1998) Morphological and rheological detection of the phase inversion of PMMA/PS polymer blends. *Polym Bull* 40:235–241
56. Vinckier I, Laun HM (1999) Manifestation of phase separation processes in oscillatory shear: droplet-matrix systems versus co-continuous morphologies. *Rheol Acta* 38:274–286
57. López-Barrón CR, Macosko CW (2012) Rheological and morphological study of cocontinuous polymer blends during coarsening. *J Rheol* 56:1315–1334
58. Li R, Yu W, Zhou C (2006) Rheological characterization of droplet-matrix versus co-continuous morphology. *J Macromol Sci Part B* 45:889–898
59. Bianchi O, Zattera AJ, Canto LB (2010) Dynamic vulcanization of hdpe/eva blend using silane. *J Elastomers Plast* 42:561–575
60. Salehiyan R, Ray SS, Bandyopadhyay J, Ojijo V (2017) The distribution of nanoclay particles at the interface and their influence on the microstructure development and rheological properties of reactively processed biodegradable polylactide/poly(butylene succinate) blend nanocomposites. *Polymers* 9:350
61. Moniruzzaman M, Winey KI (2006) Polymer nanocomposites containing carbon nanotubes. *Macromolecules* 39:5194–5205
62. Freeman GM, Marshall Jr CJ, Lackey WO, Onizawa M (2001) Hydrous clay slurry mixture containing a silane-treated clay. US 6,197,105
63. Rostami A, Masoomi M, Fayazi MJ, Vahdati M (2015) Role of multiwalled carbon nanotubes (MWCNTs) on rheological, thermal and electrical properties of PC/ABS blend. *RSC Adv* 5:32880–32890
64. Kasgoz A, Akın D, Durmus A (2012) Rheological behavior of cycloolefin copolymer/graphite composites. *Polym Eng Sci* 52:2645–2653

Publisher's note Springer Nature remains neutral with regard to jurisdictional claims in published maps and institutional affiliations.